ACS MATERIALS LETTERS

Cite This: ACS Materials Lett. 2019, 1, 64−70

www.acsmaterialslett.org

Self-Combustion Synthesis of Novel Metastable Ternary Molybdenum Nitrides

Jin Odahara,[†] Wenhao Sun,[*,‡] Akira Miura,[*,§] Nataly Carolina Rosero-Navarro,[§] Masanori Nagao,[∥] Isao Tanaka,[∥] Gerbrand Ceder,[‡,⊥] and Kiyoharu Tadanaga[§]

[†]Graduate School of Chemical Sciences and Engineering, Hokkaido University, Sapporo 060-8628, Japan

[‡]Materials Sciences Division, Lawrence Berkeley National Laboratory, Berkeley, California 94720, United States

[§]Faculty of Engineering, Hokkaido University, Sapporo 060-8628, Japan

[∥]Center for Crystal Science and Technology, University of Yamanashi, Kofu 400-8511, Japan

[⊥]Department of Materials Science and Engineering, UC Berkeley, Berkeley, California 94720, United States

Supporting Information

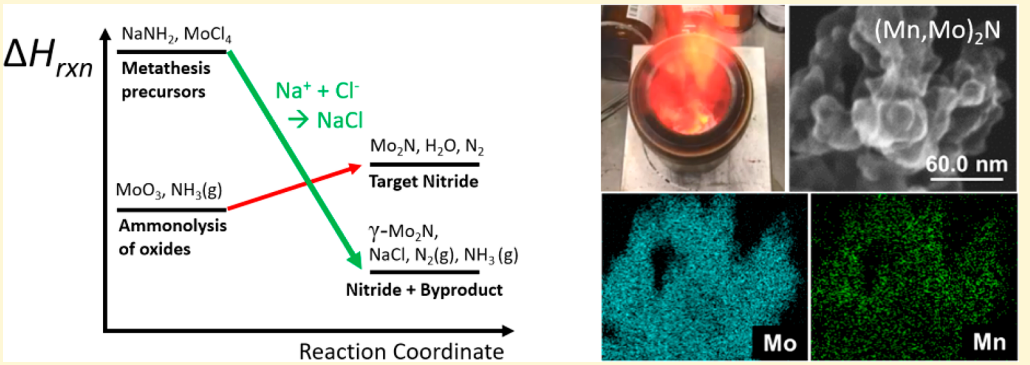

ABSTRACT: **Ternary metal nitrides are a promising class of functional materials, but their variety has been limited by the challenging nature of nitride synthesis. Here, we demonstrate a facile self-combustion synthesis route to novel ternary molybdenum nitrides. The room temperature mixing of $NaNH_2$, $MoCl_4$, and 3d transition metal chlorides, such as $MnCl_2$, $FeCl_2$, and $CoCl_2$, initiates a highly exothermic metathesis reaction, which is thermodynamically driven by the formation of stable NaCl, N_2, and NH_3 byproducts. The rapid combustion reaction yields ternary rocksalt γ-$TM_xMo_{1-x}N_{0.5}$ nanoparticles (TM = Mn, Fe, Co) in just a few seconds. We calculate from DFT that these disordered ternary molybdenum nitrides are thermodynamically stable under the high-temperatures at which they form but are remnantly metastable when quenched to ambient conditions. Introduction of Mn, Fe, and Co into γ-Mo_2N is found to change its magnetic properties and to enhance its oxygen reduction catalytic activities. Our work demonstrates self-combustion synthesis as a simple but powerful route for the realization of novel ternary intermetallic nitrides with emergent functionality.**

Ternary metal nitrides are an exciting class of functional materials[1−4] and have found applications as super hard materials,[5,6] magnetic media,[7−9] catalysts,[10,11] semiconductors,[12,13] and more. Mixed-transition metal (TM) nitrides have been reported, such as Fe_xWN_2,[14,15] $MnMoN_2$,[14] and others,[14,16] but they are relatively rare compared to ternary alkali-TM-nitrides.[1,4,17−19] Nevertheless, these early-TM nitrides, such as molybdenum nitrides, exhibit high chemical stability, which can be attributed to strong metal−nitrogen and metal−metal bonding.[20] Of the known mixed-TM nitrides, many have been synthesized by ammonolysis of oxide precursors; however, this process often requires long-term heat treatment at a narrow temperature range and a large amount of toxic ammonia gas.[14] Various other approaches have been developed for the synthesis of ternary nitrides, for example, thermal decomposition of a metal−hexamethylenetetramine complex,[21] mechanochemical alloying,[22] or solid-state reactions using NaN_3.[23] Despite these great efforts to synthesize new nitride materials, materials exploration in this space remains a challenging issue. To facilitate the discovery of new nitride materials, novel synthetic approaches are desired.

Self-combustion synthesis involves combining an alkali or alkaline earth metal compound and a metal halide, which

Received: March 4, 2019
Accepted: May 10, 2019
Published: May 10, 2019

DOI: 10.1021/acsmaterialslett.9b00057
ACS Materials Lett. 2019, 1, 64−70

drives a highly exothermic reaction that results in nanomaterials, such as nanocrystals and porous materials.[24,25] These double ion-exchange metathesis reactions are thermodynamically driven by the formation of stable byproducts,[26−32] which can facilitate the synthesis of compounds with otherwise small formation energies. To illustrate this point, Table 1 compares

Table 1. DFT-Computed Reaction Enthalpies of Oxide Ammonolysis versus Self-Combustion Metathesis Reactions for $MoN_{0.5}$

reaction type	balanced reaction	ΔH_{rxn} (kJ/$MoN_{0.5}$)
ammonolysis of metal oxides	$MoO_3 + 2NH_3(g) + \rightarrow MoN_{0.5} + 3H_2O(g) + 3/4N_2(g)$	50
combustion metathesis	$MoCl_4 + 4NaNH_2 \rightarrow MoN_{0.5} + 4NaCl + 8/3NH_3(g) + 5/12N_2(g)$	-285

the reaction thermodynamics between the ammonolysis of MoO_3 to Mo_2N[33] versus the self-combustion synthesis of Mo_2N from $NaNH_2$ and $MoCl_4$ precursors. The oxide ammonolysis reaction is enthalpically unfavorable but can be entropically-driven at high temperatures by the production of 1.75 mol of gas per Mo. On the other hand, the self-combustion metathesis reaction is highly exothermic and proceeds spontaneously even at room temperature. The resulting alkali halide salt byproducts can be removed by simply washing the reaction products with water or another polar solvent.

These self-combustion synthesis routes have been reported for several nitride compounds; for example, the reaction between $ZrCl_4$ and Li_3N produces ZrN with the formation of stable LiCl as a byproduct,[34] and we recently reported the self-combustion synthesis of barium niobium perovskite oxynitride from $Ba(OH)_2$, $NbCl_5$, and $NaNH_2$.[35] For the most part, metathesis reactions in the nitrides space have primarily focused on binary nitrides or alkali ternary nitrides, such as Li_2SiN_2.[36] Ternary mixed-transition metal ternary nitrides have not been explored as readily, despite their importance as superhard materials, superconductors, and catalysts. In this work, we report on the self-combustion synthesis of new ternary mixed-metal molybdenum nitrides in the rocksalt structure. We focus on molybdenum nitrides because molybdenum is the most effective transition metal for forming ternary metal nitrides[1] and because of the excellent performance of molybdenum nitrides in catalytic applications.[37−39] The reaction between molybdenum chloride, 3d transition metal chlorides, and sodium amide proceeded instantly, producing novel ternary molybdenum nitrides in just a few seconds. The temperature profiles of these combustion reactions exhibit rapid heating and quenching, which we demonstrate is able to produce metastable ternary $TM_xMo_{1-x}N_{0.5}$ compounds isostructural to the high-temperature γ-Mo_2N polymorph. Nitrides are the most metastable class of inorganic materials,[40] and our work here provides a simple but powerful route to this compelling class of functional materials.

Self-combustion synthesis of ternary molybdenum nitrides is initiated from a reaction between $MoCl_4$, $NaNH_2$, and 3d transition metal chlorides. Preliminary experiments in optimizing Mo−Cl precursors found that the reaction of $MoCl_5$ (Wako, 99.5%) with $NaNH_2$ at room temperature formed γ-Mo_2N and δ-MoN (Figure S1). On the other hand, a reaction with $MoCl_3$ precursors (Aldrich, 99.95%) did not initiate at room temperature. However, $MoCl_4$ was found to be an effective starting precursor for the combustion synthesis of single-phase ternary molybdenum nitrides. Note that $MoCl_4$, $MoCl_5$, and $NaNH_2$ powders are moisture-sensitive and should be handled in a glove box with inert atmosphere.

To synthesize $MoCl_4$, $MoCl_5$ and $MoCl_3$ were mixed in Ar-filled glove box. The mixture was then heated at 543 K for 12 h in a vacuum sealed glass tube and was subsequently heated at 433 K for 30 min under vacuum, resulting in $MoCl_4$. The Teflon-lined autoclave with an inner volume of 70 mL (Yanako, AD-70) was heated at 493 K overnight to remove any water before the synthesis reaction of molybdenum nitrides. Binary molybdenum nitrides were synthesized by reaction of 1 mmol of $MoCl_4$ and 10 mmol of $NaNH_2$ (Aldrich, 98%) in argon-filled glove box. For the synthesis of ternary manganese molybdenum nitride, 0.3−1.5 mmol of $MnCl_2$ (Sterm, 97%) and $MoCl_4$ was mixed in an argon-filled glove box, and placed into autoclave with 10 mmol of $NaNH_2$. Thereafter, the same procedure as described above was performed. The synthesis of molybdenum nitride with other metals was attempted in the same way employing 0.3 mmol of $CoCl_2$ (Kanto, 95%) or $FeCl_2$ (Sterm, 98%).

For the combustion synthesis reaction, black transition metal chloride powders and a magnetic stirrer were put in the autoclave, and then white $NaNH_2$ powder was added. The total mass of these powders was less than 700 mg. The mixing of $MoCl_4$, $MnCl_2$, and $NaNH_2$ initiated the combustion reaction, resulting in the formation of black powder. ***Caution!*** *An intense exothermic reaction occurs suddenly by mixing these powders. Synthesis using a large amount of the starting materials may cause a serious accident.* In the Supporting Information, we include a movie demonstrating this self-combustion reaction; although for reader's reference, the movie shows the combustion reaction in an open reaction vessel, whereas in practice, the reactions were performed in a closed autoclave. Under ambient atmosphere, the resulting products were washed with ethanol and distilled water to remove the NaCl byproducts and unreacted starting materials and, then, filtered. Then, the samples were further washed with approximately 10 mL of acetic acid (~20 vol %; diluted aqueous solution from commercial acetic acid (Kanto, 99.7 %)) and, then, washed again with ethanol and water.

Upon washing with distilled water, excess $NaNH_2$ converts into NaOH and is dissolved and washed away from the product, along with NaCl. The subsequent acetic acid treatment should dissolve residual binary manganese nitrides, which are not stable in acid.[41] On the other hand, the persistence of the ternary molybdenum nitride products after washing indicates chemical stability against water and strong bases (NaOH). Moreover, subsequent acid treatment also demonstrates stability towards weak acids. Typical reaction yields of the target ternary nitride materials were 20−30% mass based on molybdenum. Although this yield is lower than the corresponding ammonolysis reactions, the self-combustion synthesis reaction has the advantage of proceeding quickly, being relatively simple to prepare, and as we will demonstrate later, also being able to form metastable ternary nitrides.

After we washed the reaction products with distilled water and treated them with acetic acid, we characterized the black powder. Figure 1 shows the X-ray diffraction patterns of the products synthesized with various molar ratio of $MoCl_4$/$MnCl_2$, where the molar ratio of $MnCl_2/MoCl_4$ in the starting materials is defined as x. In all products, the main peaks could

DOI: 10.1021/acsmaterialslett.9b00057
ACS Materials Lett. 2019, 1, 64−70

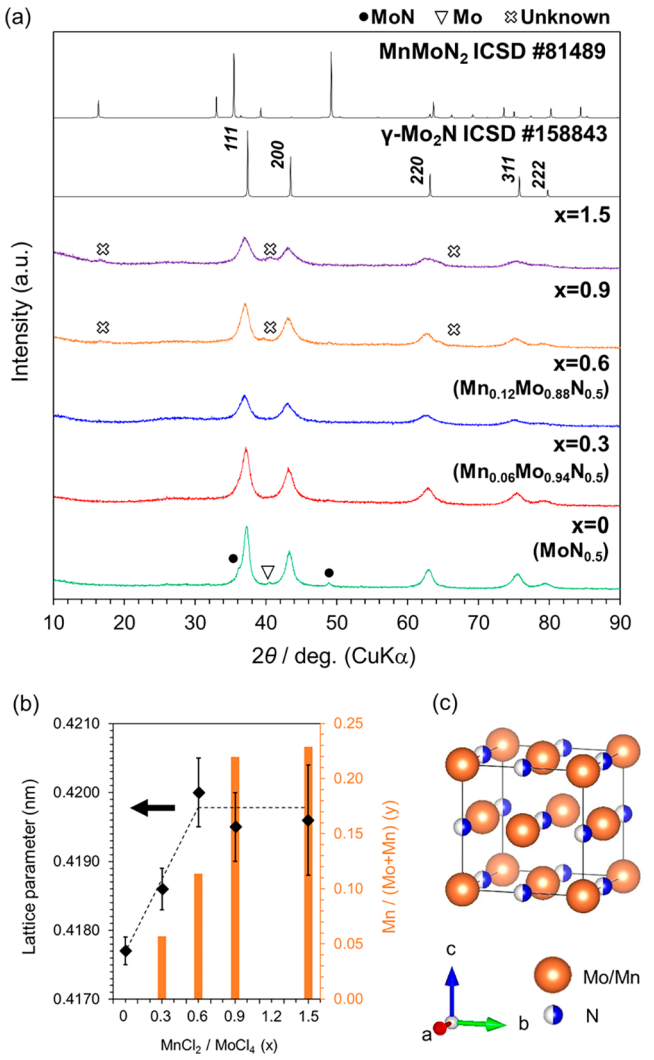

Figure 1. (a) XRD patterns of synthesized manganese molybdenum nitrides with various molar ratio of $MnCl_2/MoCl_4$ in the starting materials represented as x: The $MnCl_2/MoCl_4/NaNH_2$ ratio was 0−1.5:1:10. (b) The lattice parameters and Mn content of synthesized products from the molar ratio of $MnCl_2/MoCl_4$. The atomic ratios of the product determined by EDX, y, were shown as bars. (c) Crystal structure of synthesized $Mn_yMo_{1-y}N_{0.5}$.

be indexed as cubic γ-Mo_2N. No diffraction peaks corresponding to β-Mo_2N, $MnMoN_2$, and Mn_2N were observed. At $x = 0$, cubic γ-Mo_2N and impurities, MoN, and Mo metal, were detected. The lattice parameters of cubic γ-Mo_2N increased linearly from the precursor ratios of $x = 0$−0.6 but did not change within the error bar between $x = 0.6$ and 1.5. The Mn-composition of the products, as shown as the Mn/(Mn + Mo) ratio in Figure 1, were semi-quantitatively determined by EDX; the ratios determined by SEM-EDX agreed with those by STEM-EDX. The composition varied linearly with the lattice parameters. This linear relationship between lattice parameter and composition was further confirmed by comparing the DFT-relaxed average volume of disordered γ-$Mo_{0.875}Mn_{0.125}N_{0.5}$ against the linear interpolation between the isostructural Mo_2N and Mn_2N binaries (details in Supporting Information). This linear change in lattice parameters with composition suggests random Mn substitution for the Mo site in γ-Mo_2N at $x = 0.3$ and $x = 0.6$. Hereafter, these products with $x = 0$, 0.3, and 0.6 are expressed as $Mn_yMo_{1-y}N_{0.5}$ ($y = 0$, 0.06, and 0.12), respectively, according to the EDX analysis. We note that the Mn/(Mn + Mo) ratios in the product phase were lower than $MnCl_2/MoCl_4$ ratio in starting precursor mixtures, suggesting that there may have been unreacted manganese byproducts in the reaction, which were removed after washing with distilled water and acid treatment.

On the basis of the broad diffraction peaks, the crystalline size estimated from the Scherrer equation using the strongest peaks were 5−6 nm, although broad diffraction peaks could also arise from structural disorder in the synthesized nitrides. For $x \geq 0.9$, we observe several additional broad diffraction peaks, which cannot be assigned to the cubic phase. These diffraction peaks for $x \geq 0.9$ might possibly be attributed to the partial ordering of Mn and Mo, since the angles of unindexed peaks are close to peaks corresponding to layered $MnMoN_2$, where Mn and Mo layers stack alternatively.

The scanning transmission electron microscopy (STEM) images of $Mn_yMo_{1-y}N_{0.5}$ products ($y = 0$, 0.06, and 0.12) are shown in Figure 2a−f, taken on a Hitachi HD-2000. The size

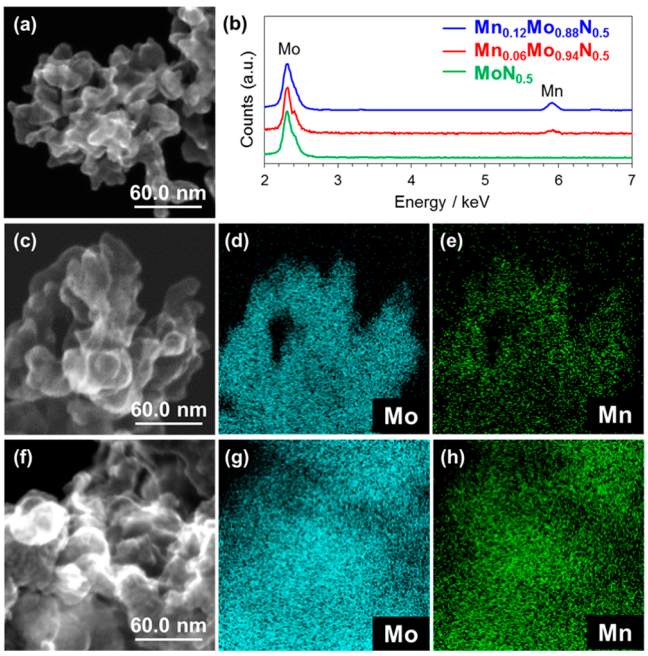

Figure 2. (a) STEM image of $MoN_{0.5}$. (b) EDX spectra of products. (c) STEM image and EDX mapping of (d) Mo and (e) Mn for $Mn_{0.06}Mo_{0.94}N_{0.5}$ sample. (f) STEM image and EDX mapping of (g) Mo and (h) Mn for $Mn_{0.12}Mo_{0.88}N_{0.5}$ sample.

of primary particles, which formed aggregates, increased with an increase in the molar ratio of $MnCl_2/MoCl_4$. These approximate particle sizes were estimated to be 20 nm for $MoN_{0.5}$, 30−40 nm for $Mn_{0.06}Mo_{0.94}N_{0.5}$, and 50 nm for $Mn_{0.12}Mo_{0.88}N_{0.5}$, respectively. Figure 2b shows the energy dispersive X-ray spectrometry (EDX) spectrum of products. The EDX peaks of Mo ($L\alpha = 2.293$ keV) and Mn ($K\alpha = 5.894$ keV) were detected for $Mn_{0.06}Mo_{0.94}N_{0.5}$ and $Mn_{0.12}Mo_{0.88}N_{0.5}$ samples. On the other hand, no manganese was detected for $MoN_{0.5}$. STEM-EDX mapping images of manganese molybdenum nitrides are shown in Figure 2c−e for $Mn_{0.06}Mo_{0.94}N_{0.5}$ and Figure 2f−h for $Mn_{0.12}Mo_{0.88}N_{0.5}$. Molybdenum and manganese showed almost similar distribution, which indicate Mn-substituted $MoN_{0.5}$.

DOI: 10.1021/acsmaterialslett.9b00057
ACS Materials Lett. 2019, 1, 64−70

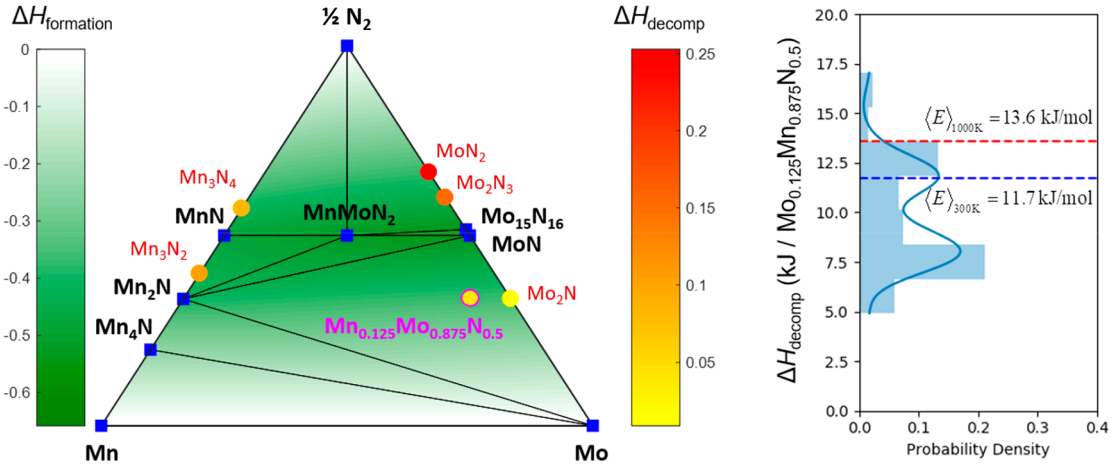

Figure 3. (a) Predicted ternary phase diagram of Mo−Mn−N space, where $Mn_{0.125}Mo_{0.875}N_{0.5}$ is highlighted in purple. Blue squares indicate stable phases; yellow-red circles are metastable phases with decomposition enthalpies noted in eV/atom, and green shading indicates formation energy of the convex hull in eV/atom. (b) Structural density of states of disordered γ-$Mn_{0.125}Mo_{0.875}N_{0.5}$. Blue and red lines indicate canonical ensemble-averaged enthalpies of the disordered phases at 300 and 1000 K, respectively.

During combustion, the temperature rises quickly and is then quenched rapidly. Thus, there is the compelling possibility that any high-temperature phases formed during combustion synthesis can be retained in a metastable state at ambient conditions. γ-Mo_2N is the high-temperature polymorph of Mo_2N, and so, the formation of the γ-phase instead of the β- or δ-phases suggests that the temperature of the self-combustion synthesis reaction exceeds 673−1123 K.[42,43] The presence of manganese could change the order/disorder transition temperature, but this effect is likely small, because of the relatively small fraction of Mn in solid-solution. Although $MnMoN_2$ is a stable phase in the predicted Mo−Mn−N phase diagram, high-temperatures promote metal reduction by evolution of gaseous N_2 driving phase equilibrium towards the nitrogen-poor intermetallic subnitrides, such as $MoN_{0.5}$.[44] It is possible that metathesis reactions carried out under high-pressures may facilitate the formation of nitrogen-rich nitrides,[45,46] which could enable interesting semiconducting properties in these ternary mixed-transition metal nitrides.

To determine the thermodynamic (meta)stability of Mn-substituted Mo_2N, we used density functional theory (DFT) to model the formation energies of disordered γ-$Mn_{0.12}Mo_{0.88}N_{0.5}$ structures. We sampled 100 randomly ordered $Mn_{0.12}Mo_{0.88}N_{0.5}$ structures on a 2 × 2 × 2 primitive rock salt structure, with a 1:7 ratio of Mn:Mo on the cation sublattice, and a 1:1 ratio of N:Vacancy on the anion sublattice. We assume that these 100 calculations statistically sample the structural density of states of the disordered structure. Because the 2 × 2 × 2 primitive lattice represents small unit cells, we compute the total energy of the disordered γ-$Mo_{0.875}Mn_{0.125}N_{0.5}$ as a microcanonical ensemble formed from a sum of smaller canonical ensembles,[47] given by the equation

$$\langle E \rangle = \sum_i \exp(-E_i/k_B T)$$

where $\langle E \rangle$ is the energy of the microcanonical γ-$Mo_{0.875}Mn_{0.125}N_{0.5}$ phase, i represents a single ordered γ-$Mo_{0.875}Mn_{0.125}N_{0.5}$ configuration on a 2 × 2 × 2 primitive cell, and E_i is the energy of that configuration.

Total energies were calculated in DFT using the Vienna ab initio software package (VASP),[48] using the projector augmented-wave method with the GGA-PBE functional. Plane-wave basis cut-off energies are set to 520 eV. The k-point densities were distributed within the Brillouin zone in a Monkhorst−Pack grid[49] and used default k-point densities in compliance with Materials Project calculation standards,[50] which were calibrated to achieve total energy convergence of better than 0.5 meV/atom. Each structure is initiated in ferromagnetic spin configurations. Phase stability calculations are then computed using the phase diagram analysis package in *pymatgen*,[51] calculated with respect to known nitride phases from the Materials Project.

The Mo−Mn−N phase diagram and a $Mo_{0.875}Mn_{0.125}N_{0.5}$ structural density of states is shown in Figure 3. The canonical ensemble-averaged formation enthalpy of $Mo_{0.875}Mn_{0.125}N_{0.5}$ is metastable by ΔH_{decomp} = 11.7 kJ/mol at room temperature with respect to Mn_2N + MoN + Mo, and metastable by ΔH_{decomp} = 13.6 kJ/mol at 1000 K. By the ideal solution model, the maximal configurational entropy of $Mo_{0.875}Mn_{0.125}N_{0.5}$ is $S_{config} = S_{anion} + S_{cation}$ = 13.4 J/(mol K). This means that disordered $Mo_{0.875}Mn_{0.125}N_{0.5}$ can be stabilized at temperatures >1000 K through its Gibbs free-energy, but it is metastable if quenched to ambient conditions, consistent with a concept of Remnant Metastability.[40] To the best of our knowledge, γ-$Mn_{0.12}Mo_{0.88}N_{0.5}$ has not been previously reported in the literature.

To compute the reaction thermodynamics of the self-combustion reactions, we used the DFT-calculated formation energy of γ-$Mn_{0.125}Mo_{0.875}N_{0.5}$, as well as the DFT formation energies for the known competing phases from the Materials Project database, and with formation energies of gaseous H_2O, NH_3, and N_2 referenced to experimental nitride formation energies,[52] using the energy referencing scheme by Wang et al.53 In the Supporting Information, we show benchmarked ammonolysis reactions, showing good agreement with calculated reaction energies and calorimetry results.

From the previously determined formation enthalpy of $Mo_{0.875}Mn_{0.125}N_{0.5}$, we compute the solid-state metathesis reaction conducted here to be highly exothermic (ΔH = −253 kJ/mol), as shown in Table 2, enabling it to proceed spontaneously at room temperature. On the other hand, the reaction enthalpy of the corresponding ammonolysis of oxides would be endothermic (ΔH = 49 kJ/mol) but could

DOI: 10.1021/acsmaterialslett.9b00057
ACS Materials Lett. 2019, 1, 64−70

Table 2. DFT-Computed Reaction Enthalpies of Oxide Ammonolysis versus Self-Combustion Metathesis Reactions for $Mo_{1-y}Mn_yN_{0.5}$

reaction type	balanced reaction	ΔH_{rxn} (kJ/ $Mo_{1-y}Mn_yN_{0.5}$)
ammonolysis of metal oxides	$1/8MnO_2 + 7/8MoO_3 + 23/12NH_3(g) \rightarrow Mn_{0.125}Mo_{0.875}N_{0.5} + 23/8H_2O(g) + 17/24\ N_2(g)$	49
combustion metathesis	$1/8MnCl_2 + 7/8MoCl_4 + 15/4NaNH_2 \rightarrow Mn_{0.125}Mo_{0.875}N_{0.5} + 15/4NaCl + 5/2NH_3(g) + 3/8N_2(g)$	-253

potentially be initiated at high-temperature by the production of H_2O and N_2 gases, providing entropy on the product side of the reaction to drive the formation of $Mo_{0.875}Mn_{0.125}N_{0.5}$. Nevertheless, between these two synthesis methods, combustion synthesis appears to be the simpler and more facile route to these novel ternary nitride compounds.

To examine the effect of Mn-substitution on the electronic structure of $MoN_{0.5}$, magnetic properties of the products were investigated by a vibrating sample magnetometer (VSM). Figure 4 shows the temperature dependence of the magnetic

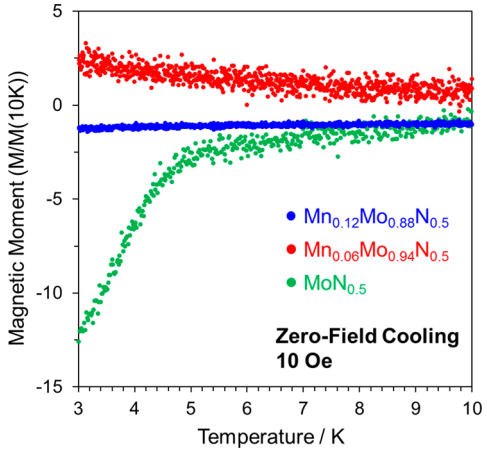

Figure 4. Temperature dependence of magnetic moment for $MoN_{0.5}$ (green), $Mn_{0.06}Mo_{0.94}N_{0.5}$ (red), and $Mn_{0.12}Mo_{0.88}N_{0.5}$ (blue).

moment of synthesized manganese molybdenum nitride $Mn_yMo_{1-y}N_{0.5}$ (y = 0, 0.06, and 0.12). The sample with $MoN_{0.5}$ showed diamagnetic signal at approximately 5 K, suggesting the appearance of superconductivity.[54] This is further evidence of γ-Mo_2N with a random occupation of nitrogen.[40] On the other hand, $Mn_{0.06}Mo_{0.94}N_{0.5}$ and $Mn_{0.12}Mo_{0.88}N_{0.5}$ did not show diamagnetic signal, indicating the disappearance of superconductivity. This change in magnetic moment indicates a modification of the electronic structure in Mn-substituted $MoN_{0.5}$.

Our synthesis of ternary molybdenum nitrides was further generalized from $MnCl_2$ to $CoCl_2$ and $FeCl_2$ (Figure S2). The lattice parameters of γ-Mo_2N phase were 0.4166(1) nm and 0.4185(1) nm for Co−Mo and Fe−Mo nitrides, respectively, which were different from that of $MoN_{0.5}$ (a = 0.4177(2) nm). Co and Fe were homogeneously distributed, suggesting the incorporation of Co and Fe into γ-Mo_2N (Figure S3). Although these syntheses were always accompanied with the formation of metals and δ−MoN and thus the synthesis of single-phase γ-Mo_2N phase remains a further challenge, this synthesis method can be expanded as a general approach for producing ternary molybdenum nitrides.

Finally, we explored the potential electrocatalytic applications of our ternary molybdenum nitrides for the oxygen reduction reaction (ORR). The ternary molybdenum nitrides synthesized in this study have <50 nm particle size and appear kinetically resistant against corrosion in alkaline solutions. Figure 5 shows the oxygen reduction reaction activity of

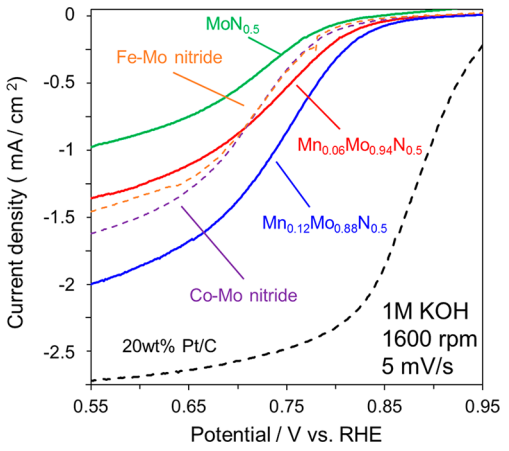

Figure 5. Linear-sweep polarization curves of products for $MoN_{0.5}$ (green), $Mn_{0.06}Mo_{0.94}N_{0.5}$ (red), $Mn_{0.12}Mo_{0.88}N_{0.5}$ (blue), Fe−Mo nitride (orange), and Co−Mo nitride (purple) recorded with a rotating disc electrode in O_2-saturated 1 M KOH solution at a sweep rate of 5 mV s^{-1}. The polarization curve of 20 wt % Pt/C is shown for comparison.

$MoN_{0.5}$ and its Mn-, Co-, and Fe-substituted ternaries in a 1 M KOH aqueous solution and also includes for reader's reference a dashed line for 20 wt % Pt/C. γ-$MoN_{0.5}$ exhibited the lowest catalytic activity, and its activity was enhanced by introducing the 3d transition metals. Catalytic activity improved with increasing Mn content, and $Mn_{0.12}Mo_{0.88}N_{0.5}$ showed the lowest overpotential and the highest current density, even though it had the largest nanoparticle size (Mo_2N ∼ 20 nm, $Mn_{0.12}Mo_{0.88}N_{0.5}$ ∼ 50 nm; Figure 2a, c, and f). Although these catalytic activities are not as high as commercial Pt/C, we demonstrate here that substitution of 3d transition metals improves the catalytic performance of γ-Mo_2N, which is likely due to modification of the electronic structure via these transition metal substitutions on the Mo site. By extending the known binary metal nitrides into ternary compositions, we can access a broader structure−property design space for enhanced materials functionality.

In summary, rapid materials preparatory methods are in great demand for scalable and sustainable materials synthesis. In this Letter, we demonstrated a facile self-combustion synthesis method for the realization of new ternary molybdenum nitrides. These reactions initiate at room temperature but rapidly reach high temperatures, and are then quenched shortly thereafter. The non-equilibrium nature of this process enables the formation of metastable disordered nitrides with emergent properties. Notably, introduction of manganese into molybdenum nitrides was found to enhance ORR activity compared to pristine γ-Mo_2N. Incorporation of iron and cobalt into γ-Mo_2N was also demonstrated, suggesting that this self-combustion synthesis method can be expanded as a general approach for the rapid exploration of novel ternary metal nitride materials. Our DFT investigation

DOI: 10.1021/acsmaterialslett.9b00057
ACS Materials Lett. 2019, 1, 64−70

yielded thermochemical insights into this highly exothermic reaction, and can be generally applied to screen for and identify similar self-combustion metathesis reactions. Finally, the combined experimental and computational investigation here offers a general paradigm for the predictive synthesis of novel functional materials.

■ ASSOCIATED CONTENT

Supporting Information

The Supporting Information is available free of charge on the ACS Publications website at DOI: 10.1021/acsmaterialslett.9b00057.

Detailed characterization details and computational methods (PDF)

Movie of the combustion synthesis reaction (MP4)

■ AUTHOR INFORMATION

Corresponding Authors

*E-mail: wenhaosun@lbl.gov.
*E-mail: amiura@eng.hokudai.ac.jp.

ORCID

Wenhao Sun: 0000-0002-8416-455X
Akira Miura: 0000-0003-0388-9696
Nataly Carolina Rosero-Navarro: 0000-0001-6838-2875
Masanori Nagao: 0000-0002-1139-7838
Isao Tanaka: 0000-0002-2736-7107
Kiyoharu Tadanaga: 0000-0002-3319-4353

Notes

The authors declare no competing financial interest.

■ ACKNOWLEDGMENTS

This research was partially supported by KAKENHI Grant Numbers 17H04950 and 17H03382, and Nissan Chemical Corporation and through the EIG CONCERT-Japan 4th Call under the Strategic International Collaborative Research Program (SICORP) of the Japan Science and Technology Agency (JST). Funding for W.S. and G.C. was provided by the US Department of Energy, Office of Science, Basic Energy Sciences, under Contract no. UGA-0-41029-16/ER392000, as a part of the DOE Energy Frontier Research Center "Center for Next Generation of Materials Design: Incorporating Metastability". STEM observation was supported by Hokkadi University microstructural characterization platform as a program of "Nanotechnology Platform" of the Ministry of Education, Culture, Sports, Science and Technology (MEXT), Japan.

■ REFERENCES

(1) Sun, W.; Bartel, C.; Arca, E.; Bauers, S.; Matthews, B.; Orvañanos, B.; Chen, B.-R.; Toney, M. F.; Schelhas, L. T.; Tumas, W.; Tate, J.; Zakutayev, A.; Lany, S.; Holder, A.; Ceder, G.A Map of the Inorganic Ternary Metal Nitrides. 2018, arXiv:1809.09202. arXiv.org e-Print archive. https://arxiv.org/abs/1809.09202.

(2) Tareen, A. K.; Priyanga, G. S.; Behara, S.; Thomas, T.; Yang, M. Mixed ternary transition metal nitrides: a comprehensive review of synthesis, electronic structure, and properties of engineering relevance. *Prog. Solid State Chem.* **2019**, *53*, 1−26.

(3) Höhn, P.; Niewa, R. Nitrides of Non-Main Group Elements. In *Handbook of Solid State Chemistry*; Dronskowski, R., Kikkawa, S., Stein, A., Eds.; Wiley-VCH: Weinheim, 2017; pp 251−359.

(4) DiSalvo, F. J.; Clarke, S. J. Ternary nitrides: a rapidly growing class of new materials. *Curr. Opin. Solid State Mater. Sci.* **1996**, *1*, 241−249.

(5) Vepřek, S.; Reiprich, S. A concept for the design of novel superhard coatings. *Thin Solid Films* **1995**, *268*, 64−71.

(6) Paseuth, A.; Yamagata, K.; Miura, A.; Higuchi, M.; Tadanaga, K. Deposition and Analysis of Al-Rich c-$Al_xTi_{1-x}N$ Coating with Preferred Orientation. *J. Am. Ceram. Soc.* **2017**, *100*, 343−353.

(7) Gudat, A.; Kniep, R.; Rabenau, A.; Bronger, W.; Ruschewitz, U. Li_3FeN_2, a ternary nitride with $1\infty[FeN_{4/2}^{3-}]$ chains: Crystal structure and magnetic properties. *J. Less-Common Met.* **1990**, *161*, 31−36.

(8) Houben, A.; Burghaus, J.; Dronskowski, R. The Ternary Nitrides $GaFe_3N$ and $AlFe_3N$: Improved Synthesis and Magnetic Properties. *Chem. Mater.* **2009**, *21*, 4332−4338.

(9) Bhattacharyya, S. Iron Nitride Family at Reduced Dimensions: A Review of Their Synthesis Protocols and Structural and Magnetic Properties. *J. Phys. Chem. C* **2015**, *119*, 1601−1622.

(10) Vaughn, D. D., II; Araujo, J.; Meduri, P.; Callejas, J. F.; Hickner, M. A.; Schaak, R. E. Solution Synthesis of Cu_3PdN Nanocrystals as Ternary Metal Nitride Electrocatalysts for the Oxygen Reduction Reaction. *Chem. Mater.* **2014**, *26*, 6226−6232.

(11) Hada, K.; Nagai, M.; Omi, S. Characterization and HDS Activity of Cobalt Molybdenum Nitrides. *J. Phys. Chem. B* **2001**, *105*, 4084−4093.

(12) Bauers, S. R.; Holder, A.; Sun, W.; Melamed, C. L.; Woods-Robinson, R.; Mangum, J.; Perkins, J.; Tumas, W.; Gorman, B.; Tamboli, A.; Ceder, G.; Lany, S.; Zakutayev, A. Ternary Nitride Semiconductors in the Rocksalt Crystal Structure. 2018, arXiv:1810.05668. arxiv.org e-Print archive. https://arxiv.org/abs/1810.05668.

(13) Arca, E.; Lany, S.; Perkins, J. D.; Bartel, C.; Mangum, J.; Sun, W.; Holder, A.; Ceder, G.; Gorman, B.; Teeter, G.; Tumas, W.; Zakutayev, A. Redox-Mediated Stabilization in Zinc Molybdenum Nitrides. *J. Am. Chem. Soc.* **2018**, *140*, 4293−4301.

(14) Bem, D. S.; LampeOnnerud, C. M.; Olsen, H. P.; zurLoye, H. C. Synthesis and structure of two new ternary nitrides: $FeWN_2$ and $MnMoN_2$. *Inorg. Chem.* **1996**, *35*, 581−585.

(15) Miura, A.; Wen, X.-D.; Abe, H.; Yau, G.; DiSalvo, F. J. Non-stoichiometric Fe_xWN_2: Leaching of Fe from layer-structured $FeWN_2$. *J. Solid State Chem.* **2010**, *183*, 327−331.

(16) Alconchel, S.; Sapina, F.; Beltran, D.; Beltran, A. Chemistry of interstitial molybdenum ternary nitrides $MnMo_3N$ (M = Fe, Co, *n* = 3; M = Ni, *n* = 2). *J. Mater. Chem.* **1998**, *8*, 1901−1909.

(17) Miura, A.; Tadanaga, K.; Magome, E.; Moriyoshi, C.; Kuroiwa, Y.; Takahiro, T.; Kumada, N. Octahedral and trigonal-prismatic coordination preferences in Nb-, Mo-, Ta-, and W-based ABX_2 layered oxides, oxynitrides, and nitrides. *J. Solid State Chem.* **2015**, *229*, 272−277.

(18) Rauch, P. E.; DiSalvo, F. J.; Brese, N. E.; Partin, D. E.; O'Keeffe, M. Synthesis and Neutron Diffraction Study of Na_3WN_3 and Na_3MoN_3. *J. Solid State Chem.* **1994**, *110*, 162−166.

(19) Yamane, H.; DiSalvo, F. J. Synthesis and crystal structure of Sr_2ZnN_2 and Ba_2ZnN_2. *J. Solid State Chem.* **1995**, *119*, 375−379.

(20) Miura, A.; Takei, T.; Kumada, N.; Wada, S.; Magome, E.; Moriyoshi, C.; Kuroiwa, Y. Bonding Preference of Carbon, Nitrogen, and Oxygen in Niobium-Based Rock-Salt Structures. *Inorg. Chem.* **2013**, *52*, 9699−9701.

(21) Wang, H.; Li, W.; Zhang, M. New Approach to the Synthesis of Bulk and Supported Bimetallic Molybdenum Nitrides. *Chem. Mater.* **2005**, *17*, 3262−3267.

(22) Jacobsen, C. J. H.; Zhu, J. J.; Lindeløv, H.; Jiang, J. Z. Synthesis of ternary nitrides by mechanochemical alloying. *J. Mater. Chem.* **2002**, *12*, 3113−3116.

(23) Wang, L.; Xian, W.; Zhang, K.; Liu, W.; Qin, H.; Zhou, Q.; Qian, Y. One-step solid state reaction for the synthesis of ternary nitrides Co_3Mo_3N and Fe_3Mo_3N. *Inorg. Chem. Front.* **2017**, *4*, 2055−2058.

DOI: 10.1021/acsmaterialslett.9b00057
ACS Materials Lett. 2019, 1, 64−70

(24) Treece, R. E.; Macala, G. S.; Kaner, R. B. Rapid synthesis of gallium phosphide and gallium arsenide from solid-state precursors. *Chem. Mater.* **1992**, *4*, 9−11.
(25) Gillan, E. G.; Kaner, R. B. Synthesis of Refractory Ceramics via Rapid Metathesis Reactions between Solid-State Precursors. *Chem. Mater.* **1996**, *8*, 333−343.
(26) Martinolich, A. J.; Neilson, J. R. Toward Reaction-by-Design: Achieving Kinetic Control of Solid State Chemistry with Metathesis. *Chem. Mater.* **2017**, *29*, 479−489.
(27) Parkin, I. *Solid State Metathesis Reaction for Metal Borides, Silicides, Pnictides and Chalcogenides: Ionic or Elemental Pathways*, 1996; Vol. *25*.
(28) Miura, A.; Takei, T.; Kumada, N. Synthesis of Wurtzite-Type InN Crystals by Low-Temperature Nitridation of $LiInO_2$ Using $NaNH_2$ Flux. *Cryst. Growth Des.* **2012**, *12*, 4545−4547.
(29) Miura, A.; Takei, T.; Kumada, N. Low-Temperature Nitridation of Manganese and Iron Oxides Using $NaNH_2$ Molten Salt. *Inorg. Chem.* **2013**, *52*, 11787−11791.
(30) Miura, A. Low-temperature synthesis and rational design of nitrides and oxynitrides for novel functional material development. *J. Ceram. Soc. Jpn.* **2017**, *125*, 552−558.
(31) Miura, A.; Lowe, M.; Leonard, B. M.; Subban, C. V.; Masubuchi, Y.; Kikkawa, S.; Dronskowski, R.; Hennig, R. G.; Abruña, H. D.; DiSalvo, F. J. Silver delafossite nitride, $AgTaN_2$? *J. Solid State Chem.* **2011**, *184*, 7−11.
(32) Todd, P. K.; Neilson, J. R. Selective formation of yttrium manganese oxides through kinetically competent assisted metathesis reactions. *J. Am. Chem. Soc.* **2019**, *141*, 1191.
(33) McKay, D.; Hargreaves, J. S. J.; Rico, J. L.; Rivera, J. L.; Sun, X. L. The influence of phase and morphology of molybdenum nitrides on ammonia synthesis activity and reduction characteristics. *J. Solid State Chem.* **2008**, *181*, 325−333.
(34) Wiley, J. B.; Kaner, R. B. Rapid Solid-State Precursor Synthesis of Materials. *Science* **1992**, *255*, 1093−1097.
(35) Odahara, J.; Miura, A.; Rosero-Navarro, N. C.; Tadanaga, K. Explosive Reaction for Barium Niobium Perovskite Oxynitride. *Inorg. Chem.* **2018**, *57*, 24−27.
(36) Song, B.; Chen, X.; Han, J.; Jian, J.; Wang, W.; Zuo, H.; Zhang, X.; Meng, S. Facile Route to Nitrides: Transformation from Single Element to Binary and Ternary Nitrides at Moderate Temperature through a New Modified Solid-State Metathesis. *Inorg. Chem.* **2009**, *48*, 10519−10527.
(37) Miura, A.; Tague, M. E.; Gregoire, J. M.; Wen, X.-D.; van Dover, R. B.; Abruña, H. c. D.; DiSalvo, F. J. Synthesis of Pt−Mo−N Thin Film and Catalytic Activity for Fuel Cells. *Chem. Mater.* **2010**, *22*, 3451−3456.
(38) Cao, B.; Neuefeind, J. C.; Adzic, R. R.; Khalifah, P. G. Molybdenum nitrides as oxygen reduction reaction catalysts: structural and electrochemical studies. *Inorg. Chem.* **2015**, *54*, 2128−36.
(39) Cao, B.; Veith, G. M.; Neuefeind, J. C.; Adzic, R. R.; Khalifah, P. G. Mixed close-packed cobalt molybdenum nitrides as non-noble metal electrocatalysts for the hydrogen evolution reaction. *J. Am. Chem. Soc.* **2013**, *135*, 19186−92.
(40) Sun, W.; Dacek, S. T.; Ong, S. P.; Hautier, G.; Jain, A.; Richards, W. D.; Gamst, A. C.; Persson, K. A.; Ceder, G. The thermodynamic scale of inorganic crystalline metastability. *Sci. Adv.* **2016**, *2*, e1600225−e1600225.
(41) Lyutaya, M. D.; Goncharuk, A. B. Manganese nitrides. *Powder Metall. Met. Ceram.* **1977**, *16*, 208−212.
(42) Ettmayer, P. Das System Molybdän-Stickstoff. *Monatsh. Chem.* **1970**, *101*, 127−140.
(43) Jehn, H.; Ettmayer, P. The molybdenum-nitrogen phase diagram. *J. Less-Common Met.* **1978**, *58*, 85−98.
(44) Sun, W.; Holder, A.; Orvañanos, B.; Arca, E.; Zakutayev, A.; Lany, S.; Ceder, G. Thermodynamic Routes to Novel Metastable Nitrogen-Rich Nitrides. *Chem. Mater.* **2017**, *29*, 6936−6946.
(45) Lei, L.; Yin, W.; Jiang, X.; Lin, S.; He, D. Synthetic Route to Metal Nitrides: High-Pressure Solid-State Metathesis Reaction. *Inorg. Chem.* **2013**, *52*, 13356−13362.
(46) Horvath-Bordon, E.; Riedel, R.; Zerr, A.; McMillan, P. F.; Auffermann, G.; Prots, Y.; Bronger, W.; Kniep, R.; Kroll, P. High-pressure chemistry of nitride-based materials. *Chem. Soc. Rev.* **2006**, *35*, 987−1014.
(47) Yang, K.; Oses, C.; Curtarolo, S. Modeling Off-Stoichiometry Materials with a High-Throughput Ab-Initio Approach. *Chem. Mater.* **2016**, *28*, 6484−6492.
(48) Kresse, G.; Furthmüller, J. Efficient iterative schemes for ab initio total-energy calculations using a plane-wave basis set. *Phys. Rev. B: Condens. Matter Mater. Phys.* **1996**, *54*, 11169−11186.
(49) Monkhorst, H. J.; Pack, J. D. Special points for Brillouin-zone integrations. *Phys. Rev. B* **1976**, *13*, 5188−5192.
(50) Jain, A.; Ong, S.P.; Hautier, G.; Chen, W.; Richards, W.D.; Dacek, S.; Cholia, S.; Gunter, D.; Skinner, D.; Ceder, G.; Persson, K.A. Commentary: The Materials Project: A materials genome approach to accelerating materials innovation. *APL Mater.* **2013**, *1*, 011002.
(51) Ong, S. P.; Richards, W. D.; Jain, A.; Hautier, G.; Kocher, M.; Cholia, S.; Gunter, D.; Chevrier, V. L.; Persson, K. A.; Ceder, G. Python Materials Genomics (pymatgen): A robust, open-source python library for materials analysis. *Comput. Mater. Sci.* **2013**, *68*, 314−319.
(52) Elder, S. H.; DiSalvo, F. J.; Topor, L.; Navrotsky, A. Acta Crystallographica Section B: Structural ScienceThermodynamics of ternary nitride formation by ammonolysis: application to lithium molybdenum nitride ($LiMoN_2$), sodium tungsten nitride (Na_3WN_3), and sodium tungsten oxide nitride (Na_3WO_3N). *Chem. Mater.* **1993**, *5*, 1545−1553.
(53) Wang, L.; Maxisch, T.; Ceder, G. Oxidation energies of transition metal oxides within the GGA+U framework. *Phys. Rev. B: Condens. Matter Mater. Phys.* **2006**, *73*, 195107.
(54) Matthias, B. T.; Hulm, J. K. A Search for New Superconducting Compounds. *Phys. Rev.* **1952**, *87*, 799−806.

DOI: 10.1021/acsmaterialslett.9b00057
ACS Materials Lett. 2019, 1, 64−70